# Preparation of glass-ceramics in the MgO-Al$_2$O$_3$-SiO$_2$ system via low-Temperature combustion synthesis technique

Y. He[1], J. M. Guo[2], G. W. Zhang[1], X. L. Chen[*1],
J. C. Zhang[1], Z. L. Huang[1], G. Y. Liu[1], Q. Cai[1]

[1]School of Science, Honghe University, Mengzi 661100, China
[2]Joint Research Centre for International Cross-border Ethnic area Biomass Clean Utilization in
Yunnan Province, Yunnan Minzu University, Kunming 650500, China

## Abstract

MgO-Al$_2$O$_3$-SiO$_2$ (MAS) glass powders have been successfully synthesized by means of the low-temperature combustion technique using magnesium nitrate, aluminium nitrate and silicic acid as raw materials, and urea as fuel. The sintering behavior, crystallization process and dielectric properties of the MAS were investigated with DCS, XRD, TMA and SEM techniques. The results indicate that the sintering temperature of the as-prepared glass powders decreased with the addition of B$_2$O$_3$ and only α-cordierite was precipitated as a main crystal phase, i.e. without μ-cordierite, for the glass powders heated at 1000 °C. Moreover, the as-prepared α-cordierite exhibited a dense microstructure, the additive (B$_2$O$_3$ 2.5 %) reducing the crystallization temperature of α-cordierite phase from 1050 °C to 900 °C. The obtained cordierite-based glass-ceramics (sintered at 950 °C and 1000 °C) have a low dielectric constant (4.00 ~ 4.03 at 1 MHz), a low dielectric dissipation factor (≈ 0.003) and high sintering density (which is up to 98 % of the theoretical density). The properties of as-prepared MAS satisfy all requirements of a material for electronic packaging, making it a promising candidate for application as electronic packaging.

*Keywords: Cordierite-based glass ceramics, low-temperature combustion synthesis, crystallization process, sintering behavior, electronic packaging*

## I. Introduction

Cordierite (2MgO·2Al$_2$O$_3$·5SiO$_2$) (MAS) and cordierite-based glass ceramics, which are well-known for their favorable properties, e.g. good mechanical properties (strength of ~ 250 MPa and modulus of ~ 150 GPa), low dielectric constant, low coefficient of thermal expansion, high thermal and chemical stability, are promising materials for cook-top panels or large segmented telescopes[1], and have potential for application as refractory systems[2], and honeycomb catalytic supports[3]. More importantly, if tailored, their low densification temperature, dielectric constant, better chemical durability and thermal expansion coefficients can make them useful materials for electronic packaging[4, 5].

However, the properties of glass-ceramics are dependent on their method of synthesis, chemical composition and thermal history. Several techniques have been devised to synthesize ceramics like solid-state reaction[6], polyacrylamide gels[7], sol-gel-based processes[8, 9], sintering and crystallization from the vitreous state[10], and laser fusing[11, 12]. Despite these successes in preparing cordierite ceramic, most of the sequential methods involve complicated procedures or rigorous conditions, and even worse, the obtained cordierite powders have a high melting temperature. For example, cordierite ceramic obtained based on the solid state reaction of the component oxides MgO, Al$_2$O$_3$ and SiO$_2$ or based on glass recrystallization requires a high temperature, and cannot be co-fired with copper (1083 °C), silver (961 °C) or gold (1061 °C) [13, 14]. The sol-gel process has also been widely studied to synthesize cordierite ceramic in recent years, but the method is expensive, involves a complicated process and makes high environment demands[15]. C. Oelgardt *et al.* investigated transparent microspheres in the K$_{0.5}$Na$_{0.5}$NbO$_3$ system [11] and the eutectic composition Al$_2$O$_3$-Y$_2$O$_3$-ZrO$_2$ [12] prepared by means of laser fusing with a CO$_2$ laser. Although this new technique offers some advantages (i.e. high-purity energy source, defined beam profile) and improves the mechanical properties (i.e. fracture toughness and strength, especially in the high temperature range[16]), the technique involves complicated procedures and needs a high calcined temperature before laser fusing.

Compared with other synthetic methods, a solution combustion synthesis method is a simple and direct method to synthesize cordierite powders. It is outstanding because it is not only time- and energy-saving and requires simple equipment and cheap reagents, the powders exhibit a lower sintering temperature. The low-temperature combustion synthesis technique (LCS) is a synthesis procedure based on an oxidation-reduction reaction between

soluble precursor salts (oxidizers) and sacrificial, most often carbonaceous, compounds (fuels). Owing to fast evaporation of the solvent and release of a large volume of thermolytic gaseous products, a voluminous porous product is obtained. The product consists of loosely packed homogeneous crystallites with uniform, usually nanometric particle size. Recently, we have reported modified LCS to fabricate $LiNi_{0.5}Mn_{1.5}O_4$ lithium-ion battery cathodes by combining combustion synthesis[17]. Hong[18] has synthesized cordierite-based glass powders with $Mg(NO_3)_2 \cdot 6H_2O$, $Al(NO_3)_3 \cdot 9H_2O$, $SiO_2$ as material, $CO(NH_2)_2$ used as fuel and $NH_4NO_3$ used as a combustion aid, but these powders also have a high sintering temperature (1400 °C) and low sintering density (86 % of theoretical density).

Additionally, it is also important to obtain cordierite-based glass powders with a low melting temperature by adding nucleating agents or sintering aids[19]. Meanwhile, annealing the $MgO$-$Al_2O_3$-$SiO_2$ system without any additives leads to surface crystallization. The addition of nucleating agents leads to volume-crystallized and fine-grained glass-ceramics[20]. Hunger *et al.*[21] reported on the preparation of glass-ceramics in the system of $MgO/Al_2O_3/SiO_2$ with $TiO_2$ and $ZrO_2$ as nucleating agent. The glasses were annealed at lower temperature, and after annealing at 1100 °C microhardness up to 12.3 GPa and Young's modulus up to 152 GPa were reached. In this paper, 2.5 % $B_2O_3$ was used as an additive to obtain glass-ceramics with a low melting temperature, low dielectric constant, and high sintering density.

In this paper, cordierite powders were synthesized by means of LCS using 2.5 % $B_2O_3$ as nucleating agent, but $H_2SiO_3$ instead of $SiO_2$ was used to introduce Si source, and a non-stoichiometric composition ($MgO$ 16.8 %, $Al_2O_3$ 27.4 % and $SiO_2$ 55.8 % in wt%) instead of a stoichiometric composition ($MgO$ 13.8 %, $Al_2O_3$ 34.9 % and $SiO_2$ 51.3 % in wt%) was used to improve sintering characteristics at lower temperature.

## II. Experimental

### (1) Reagents

$Mg(NO_3)_2 \cdot 6H_2O$, $Al(NO_3)_3 \cdot 9H_2O$, $H_2SiO_3$, $CO(NH_2)_2$, $NH_4NO_3$ were purchased from Sinopharm Chemical Reagent Co. Ltd. (Shanghai, China). All other chemicals used were of analytical reagent grade. Ultrapure water was obtained with a Milli-Q plus water purification system (Millipore Co. Ltd., USA) (18 M$\Omega$).

### (2) Apparatus

The surface areas and average diameter of the as-prepared powders were measured with a Quantachrome NOVA Automated Gas Sorption System (NOVA 4000) and laser particle size analyzer (Master Sizer 2000), and their microstructure was analyzed with a scanning electron microscope (SEM) (JSM-6460 LV), the surface of the samples (Fig. 5 (a, c)) was polished to under 1 μm and eroded with HF (4 wt%) for 60 s. The longitudinal sections of the samples are fracture surfaces (Fig. 5 (b, d)). These were then sputtered with a gold coating, so that the crystal morphology could be easily observed. The sintering behavior and the crystallization process of the as-prepared powders were investigated with TMA (NETZSCH DIL 402 PC) and differential thermal analysis (DSC, NETZSCH STA 409 PC/PG), the heating rate was 30 K min$^{-1}$. x-ray powder diffraction (XRD) patterns of the as-prepared sintered pellets were recorded with a BRUKER D8 Advance at 30 mA and 40 kV using Cu K$\alpha$ radiation. The densities of sintered specimens were measured with the liquid displacement method (Archimedes method). The sintered pellets were painted with silver paste on two surfaces and fired to form an electrode, then a HP4278A capacitance meter was used to measure the dielectric properties of the samples.

### (3) Experiment procedure

The stoichiometry of the redox mixtures used for combustion were calculated using the total oxidizing and reducing valencies of the components that serve as numerical coefficients for stoichiometric balance so that the equivalence ratio ($\Psi_e$) is in unity and the energy released by combustion is at a maximum. The $H_2SiO_3$ was crushed and sieved through a 200 mesh prior to the synthesis of the glass powders. Batches of 533.21 g with the compositions ($Mg(NO_3)_2 \cdot 6H_2O$, $Al(NO_3)_3 \cdot 9H_2O$, $H_2SiO_3$, $CO(NH_2)_2$, $NH_4NO_3$($MgO$ 16.8 %, $Al_2O_3$ 27.4 % and $SiO_2$ 55.8 % in wt%)) given in Table 1 were of mixed uniformity and formed a homogeneous slurry with the addition of a moderate quantity of deionized water, which was ground by means of ball milling. The slurry was concentrated by heating to form a viscous liquid with foam in the electric furnace, then transferred quickly into a muffle furnace at 500 °C, the mixture was decomposed and ignited, resulting in incandescent combustion. The as-prepared glass powders are homogeneous particles.

**Table 1:** The ingredients of the glass powders.

| Ingredients | M/g·mol$^{-1}$ | Purity level | mass/g | Composition |
|:---:|:---:|:---:|:---:|:---:|
| $Mg(NO_3)_2 \cdot 6H_2O$ | 375.13 | AR | 107.58 | $MgO$ (16.8 wt%) |
| $Al(NO_3)_3 \cdot 9H_2O$ | 256.41 | AR | 202.94 | $Al_2O_3$ (27.4 wt%) |
| $H_2SiO_3$ | 78.10 | AR | 73.00 | $SiO_2$ (55.8 wt%) |
| $CO(NH_2)_2$ | 60.06 | AR | 149.69 | fuel (0 wt%) |

The stoichiometry of the redox mixtures used for combustion were calculated using the total oxidizing and reducing valencies of the components that serve as numerical coefficients for stoichiometric balance so that the equivalence ratio ($\Psi_e$) is in unity and the energy released by combustion is at a maximum. The H$_2$SiO$_3$ was crushed and sieved through a 200 mesh prior to the synthesis of the glass powders. Batches of 533.21 g with the compositions (Mg(NO$_3$)$_2$·6H$_2$O, Al(NO$_3$)$_3$·9H$_2$O, H$_2$SiO$_3$, CO(NH$_2$)$_2$, NH$_4$NO$_3$(MgO 16.8 %, Al$_2$O$_3$ 27.4 % and SiO$_2$ 55.8 % in wt%)) given in Table 1 were of mixed uniformity and formed a homogeneous slurry with the addition of a moderate quantity of deionized water, which was ground by means of ball milling. The slurry was concentrated by heating to form a viscous liquid with foam in the electric furnace, then transferred quickly into a muffle furnace at 500 °C, the mixture was decomposed and ignited, resulting in incandescent combustion. The as-prepared glass powders are homogeneous particles.

The powders were ground and sieved through a 200-mesh to produce glass powder, and calcined at 600 °C for 2 h to remove residual organic compound. Two samples, with additive (B$_2$O$_3$ 2.5 %) or not, are referred to as S$_B$ and S$_0$, respectively. The S$_0$ and S$_B$ were uniaxially pressed to form pellets and sintered at different temperatures (850 °C, 900 °C, 950 °C, 1000 °C, 1050 °C, 1100 °C and 1200 °C) for 6 h.

## III. Results and Discussion

### (1) The glass powders prepared with the low-temperature combustion technique

The porous glass powders were prepared successfully by means of LCS, the synthesis procedure based on an oxidation-reduction reaction between the precursor salts (Mg(NO$_3$)$_2$·6H$_2$O, Al(NO$_3$)$_3$·9H$_2$O, H$_2$SiO$_3$) and fuels (CO(NH$_2$)$_2$). According to the principle of propellant chemistry, the reaction equation of LCS process can be expressed as follows:

$$6Mg(NO_3)_2+12Al(NO_3)_3+40CO(NH_2)_2+15H2SiO_3=$$
$$3Mg_2Al_4Si_5O_{18}+40CO_2+95H_2O+64N_2$$
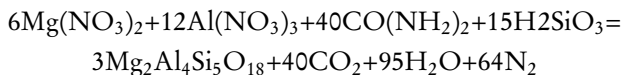
A great deal of gas such as CO$_2$, N$_2$ and H$_2$O was released from the combustion reaction process, so the as-prepared powders contained lots of holes (Fig. 1), resulting in a large surface area (186 m$^2$·g$^{-1}$) and an average diameter of 5.6 μm, leading to better sintering characteristics.

### (2) Crystallization process

The DSC curves of the powder S$_0$ and S$_B$ are shown in Fig. 2. In the sample S$_0$,the two exothermic peaks around 1000 °C and 1150 °C correspond to the crystallization of two cordierite phases. It indicates that the crystallization process of the MAS experiences a two-step process, the μ-cordierite phase was first crystallized from the glass state, and then transformed into α-cordierite phase, which matches well with the XRD pattern in Fig. 3(a). In the sample S$_B$, there is only one broadened exothermic peak around 1030 °C. It corresponds to the μ-cordierite phase and α-cordierite phase which were crystallized from glass state at the same time, which also can be proved by XRD pattern in Fig. 3(b).
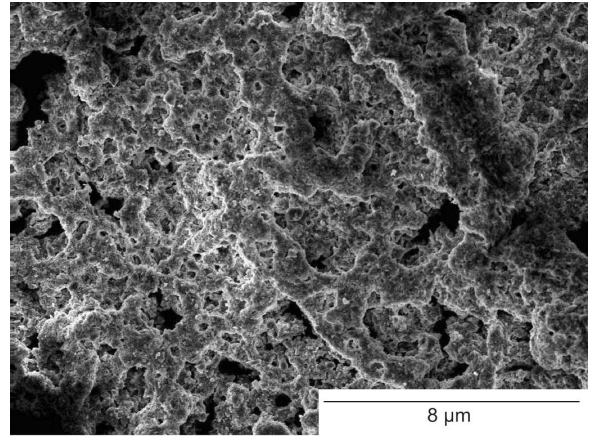


**Fig. 1:** SEM micrograph of the glass powders produced with the low-temperature combustion synthesis technique.
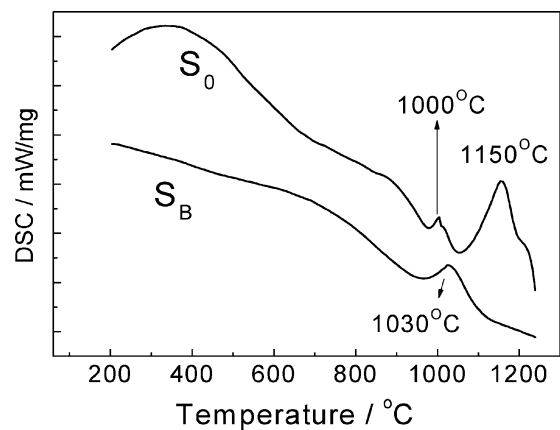


**Fig. 2:** DSC curve of MAS glass powders.

The appearance and properties of glass-ceramics are directly related to the crystallization of glass. To further identify formed phases of the S$_0$ and S$_B$, XRD experiments were conducted for the phase analysis of the as-prepared samples. XRD analysis (Fig. 3) reveals the presence of μ-cordierite and/or α-cordierite phases in the glass matrix about the S$_0$ and S$_B$ sintered at various temperatures for 6 h. In Fig. 3(a), it is clearly seen that the S$_0$ is an amorphous phase when sintered at the temperature below 850 °C. But the μ-cordierite phase was firstly crystallized from the glass state at 900 °C, then transformed into α-cordierite phase at the temperature above 1050 °C. The α-cordierite single crystal phase was obtained at 1200 °C and the temperature was lower than others in the literature [18]. Therefore, the crystallization process can be considered as the following sequence: amorphous → μ-cordierite → α-cordierite. However, the higher crystallization and transformation temperatures shown in DSC than in XRD, which may be attributed to the higher heating rate during the process of thermal analysis

In Fig. 3(b), it is also seen that the S$_B$ is an amorphous phase when the samples were sintered below 850 °C, but the μ-cordierite phase and α-cordierite phase were crystallized from the glass state at the same time at 900 °C, and transformed into α-cordierite phase after the sintered temperature above 950 °C. α-cordierite single crystal phase was obtained at 1000 °C and XRD peak intensity increased abruptly as the sintering temperature

increased from 950 °C to 1000 °C. The additive ($B_2O_3$ 2.5 %) reduces the sintering temperature needed to obtain cordierite-based glass powders and notably improves the formation of α-cordierite phase from μ-cordierite phase or glass state. Furthermore, the $B_2O_3$ lowers the crystallization temperature of the α-cordierite phase from 1050 °C to 900 °C, as the addition of $B_2O_3$ can enhance the heterogeneous nucleation of α-cordierite phase.
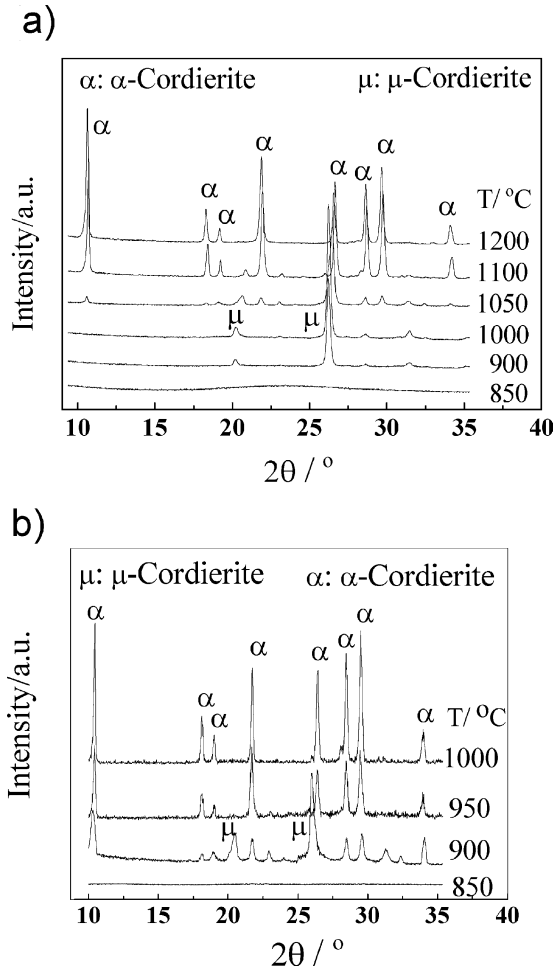
**a)**



**b)**



**Fig. 3 :** XRD patterns of the samples sintered at different temperatures for 6 h. (a) $S_0$; (b) $S_B$.

Fig. 4 shows XRD images of $S_B$ sintered at 1000 °C for 2, 4, 6 and 8 h, respectively, which confirm that crystals phases form and transform during different sintering times. It can be seen that α-cordierite phase was crystallized from the glass state at 1000 °C for the all sintering times, and the diffraction peak intensity of the α-cordierite phase increases with the sintering times. The formation of α-cordierite phase was more obvious at 6 h, but for the $S_B$ sintered for 8 h, the diffraction peak intensity of α-cordierite phase did not increase further. Thus, 6 h was chosen as the optimal sintering time.

The morphology of the $S_0$ and $S_B$ has been examined by means of SEM. Fig. 5 (a, b) shows SEM micrographs of the ceramic $S_0$ sintered at 1000 °C. The grains precipitated with 40 ~ 120 nm are α-cordierite existing mainly on the glass powder surface, as observed in Fig. 5 (a), which have been identified in the XRD results in Fig. 3. To reveal the detailed interior phase of the bulk ceramic $S_0$, the corresponding longitudinal section of sintered pellets is

shown in Fig. 5 (b), where no α-cordierite clustering was detected. This suggests that the α-cordierite phase crystallized mainly via surface nucleation without any additives. However, the addition of nucleating agents ($B_2O_3$ 2.5 %) leads to bulk crystallized and fine-grained glass-ceramics in Fig. 5 (c, d), which exhibited a dense microstructure. The α-cordierite with a particle size of 80 ~ 200 nm was homogeneously distributed on the surface of $S_B$ (Fig. 5(c)), and provided by more intensive crystallization and presence of α-cordierite phase on the longitudinal section of the representative sample (Fig. 5 (d)). This suggests that the added $B_2O_3$ may act as a nucleating agent initially precipitated as sites for heterogeneous phase nucleation.

### (3) Sintering characteristics

Fig. 6 shows the sintering shrinkage curves of the samples $S_0$ and $S_B$. It is clearly seen that the densification behavior of $S_0$ starts at about 800 °C and is completed at around 1015 °C. Compared with the sample $S_0$ without $B_2O_3$, the densification behavior of $S_B$ starts about 760 °C and is complete at around 1000 °C. It can be concluded that adding $B_2O_3$ could notably reduce the densification temperature of the sample, promoting sintering at an even lower temperature. The densities of the ceramics sintered at different temperatures were measured with the Archimedes method. The density of the ceramic $S_B$ sintered at 1000 °C is 2.461 $g \cdot cm^{-3}$, which is up to 98 % of the theoretical density (2.512 $g \cdot cm^{-3}$) of α-cordierite [18]. This means the glass powders synthesized with the low-temperature combustion technique have good low-temperature sintering characteristics. Three interpretations can be proposed for the sintering characteristics: (i) Using pectic silicic acid slurry instead of silicon dioxide is conducive to obtaining glass powders with a low sintering temperature; (ii) The sintering of a cordierite glass composition containing more MgO and less $Al_2O_3$ is easier than sintering a stoichiometric composition [22]; (iii) A great deal of gas such as $CO_2$, $N_2$ and $H_2O$ is released from the combustion reaction process, resulting in the porous glass powders with a large surface area (186 $m^2 \cdot g^{-1}$) and leads to better sintering characteristics.
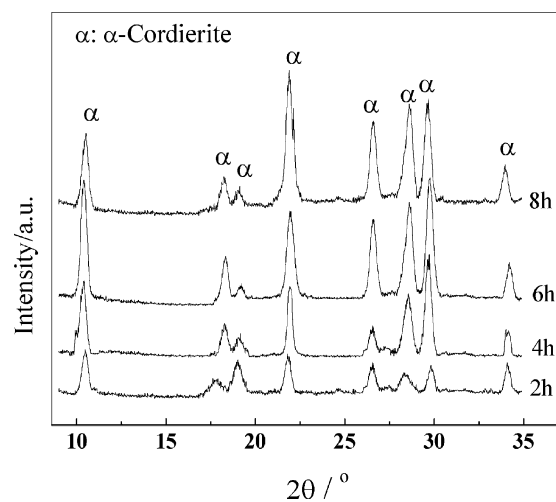


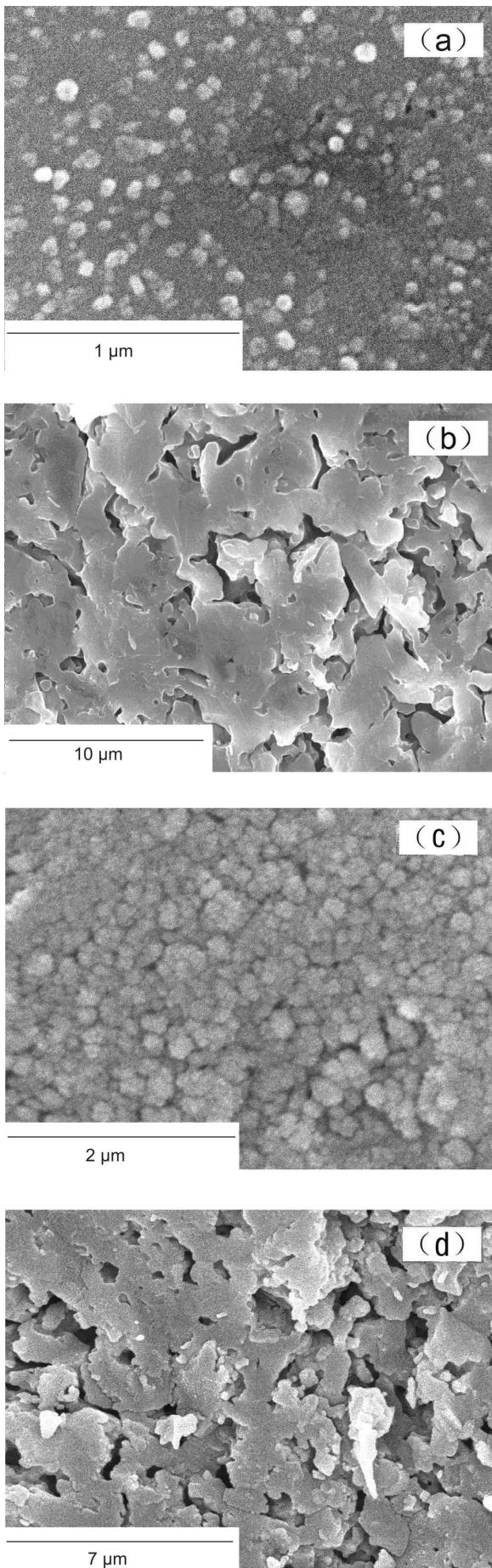**Fig. 4 :** XRD patterns of $S_B$ sintered at 1000 °C for different times.
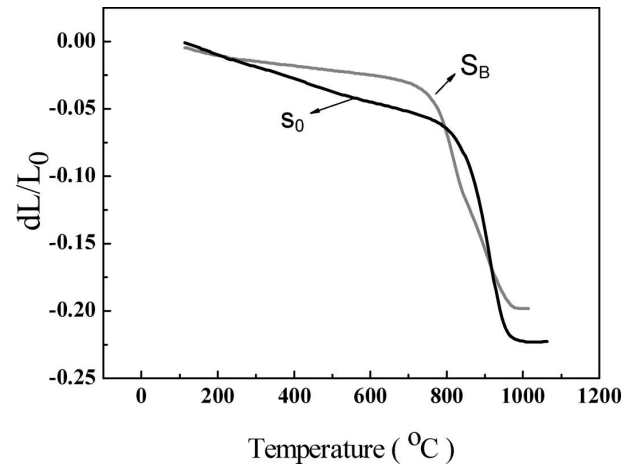
**Fig. 6 :** Shrinkage curves of the sample S$_0$ and S$_B$.

### (4) Dielectric properties

It is well-known that if glass-ceramic is to be used as a material for electronic packaging, certain requirements need to be met: the material must be sintered and densified at about 1000 °C (so it can be co-sintered with the copper internal electrode), the dielectric constant must be less than 5, the electric insulation performance and thermal expansion coefficients must be good and so on[23, 24]. The dielectric constant, dielectric dissipation factor and other primary properties of the sample S$_B$ sintered at 950 °C and 1000 °C are listed in Table 2. It can be seen that the α-cordierite-based glass-ceramic has a low dielectric constant, low dissipation factor and high electric resistivity, making it suitable for electronic packaging.

**Table 2:** The main properties of cordierite-based glass ceramics.

| Sample code | S$_B$ | |
|---|---|---|
| Sintering temperature/°C | 950 °C | 1000 °C |
| Crystal phase | α | α |
| Density/g·cm$^{-3}$ | 2.479 | 2.461 |
| Dielectric constant (1MHz) | 4.030 | 4.000 |
| Dissipation factor (1MHz) | 0.003 | 0.002 |
| Resistivity $\varrho \times 10^{12}$/Ω·cm | 1.630 | 3.560 |

### IV. Conclusions

From the above experimental results, the conclusion can be summarized as follows: as-prepared glass powders with excellent properties have been synthesized by means of the low-temperature combustion technique using urea as fuel, nitrates as oxidizer and silicic acid as the silica source; the powders can be sintered at temperatures lower than 1000 °C. During the sintering process, the μ-cordierite phase was first crystallized from glass state, and then transformed into α-cordierite phase. For the MAS glass with the addition of 2.5 % B$_2$O$_3$ sintered at 1000 °C, α-cordierite



**Fig. 5 :** SEM micrographs of the ceramic S$_0$ and S$_B$ sintered at 1000 °C (a) the surface of S$_0$; (b) the longitudinal section of S$_0$; (a) the surface of S$_B$; (b) the longitudinal section of S$_B$.

clustering homogeneously distributed in the dense glass matrix was found. More importantly, the $B_2O_3$ additive reduces the crystallization temperature of the α-cordierite phase from 1050 °C to 900 °C and notably improves the formation of α-cordierite phase from μ-cordierite phase or glass state. Furthermore, the obtained cordierite-based glass-ceramics have a low dielectric constant, high electric resistivity and low sintering temperature, making them suitable for use as electronic packaging.

## References

[1] Pannhorst, W.: Recent developments for commercial applications of low expansion glass ceramics, *Glass Technol. – Part A,* **45**, 51 – 53, (2004).

[2] Prasad, A., Basu, A.: Dielectric and impedance properties of sintered magnesium aluminum silicate glass-ceramic, *J. Adv. Ceram.,* **2**, 71 – 78, (2013).

[3] González-Velasco, T.R., Ferret, R., López-Fonseca, R., Gutiérrez-Ortiz, M.A.: Influence of particle size distribution of precursor oxides on the synthesis of cordierite by solid-state reaction, *Powder Technol.,* **153**, 34 – 42, (2005).

[4] Zhang, P.X., Hui, W.B., Zhang, Y., Ren, X.Z., Zhang, D.Y.: Molecular dynamics simulation for the rapid solidification process of $MgO$-$Al_2O_3$-$SiO_2$ glass-ceramics, *J. Non-Cryst. Solids,* **358**, 1465 – 1473, (2012).

[5] Hunger, A., Carl, G., Rüssel, C.: Formation of nano-crystalline quartz crystals from $ZnO/MgO/Al_2O_3/TiO_2/ZrO_2/SiO_2$ glasses, *Solid State Sci.,* **12**, 1570 – 1574, (2010).

[6] Shieh, Y.N., Rawlings, R.D., West, R.F.: Constitution of laser melted $Al_2O_3$-$MgO$-$SiO_2$ ceramics, *Mater. Sci. Technol.,* **11**, 863 – 869, (1995).

[7] Douy, A.: Organic gels in the preparation of silico-aluminate powders. II. Cordierit, *J. Eur. Ceram. Soc.,* **7**, 397 – 403, (199l).

[8] Guo, X.Z., Nakanishi, K., Kanamori, K., Zhu, Y., Yang, H.: Preparation of macroporous cordierite monoliths via the sol-gel process accompanied by phase separation, *J. Eur. Ceram. Soc.,* **34**, 817 – 823, (2014).

[9] Komarneni, S.: Some significant advances in sol-gel processing of dense structural ceramics, *J. Sol-Gel Sci. Technol.,* **6**, 127 – 138, (1996).

[10] Winter, W.: Sintering and crystallization of volume- and surface-modified cordierite glass powders, *J. Mater. Sci.,* **32**, 1649 – 1655, (1997).

[11] Oelgardt, C., Günster, J., Heinrich J.G.: Characterization of the crystallization behavior of laser-fused transparent microspheres with the eutectic composition $Al_2O_3$-$Y_2O_3$-$ZrO_2$ (AYZ), *J. Ceram. Sci. Tech.* **02**, 103 – 110, (2011).

[12] Hmood, F.J., Oelgardt, C., Görke, R., Heinrich J.G.: Preparation of transparent microspheres in the system $K_{0.5}Na_{0.5}NbO_3$ by laser fusing, *J. Ceram. Sci. Tech.,* **04**, 41 – 48, (2013).

[13] Li, Z., Wu, J.F., Song, L., Huang, Y.Q.: Effect of composition on sinter-crystallization and properties of low temperature co-fired α-cordierite glass-ceramics, *J. Eur. Ceram. Soc.,* **34**, 3981 – 3991, (2014).

[14] Choi, Y-J., Park, J-H,. Park, J-H., Nahm, S., Park, J-G.: Middle-and high-permittivity dielectric compositions for low-temperature co-fired ceramics, *J. Eur. Ceram. Soc.,* **27**, 2017 – 2024, (2007).

[15] Chen, G.H.: A New Low-temperature Co-fired Cordierite-based Glass-ceramics, *Piezoelectrics & Acoustooptics,* **04**, 421, (2005).

[16] Psator, J.Y., LLorca, J., Martín, A., Pena, J.I., Oliete, P.B.: Fracture toughness and strength of $Al_2O_3$-$Y_3Al_5O_{12}$ and $Al_2O_3$-$Y_3Al_5O_{12}$-$ZrO_2$ directionally solidified eutectic oxides up to 1900 K, *J. Eur. Ceram. Soc.,* **28**, 2345 – 2351, (2008).

[17] Kong, X., Sun, H.Y., Wang, Q.B., Yi, Z.Z., Wang, B.S., Liu, G.Y.: Improvement in the electrochemical properties of Li-$Ni_{0.5}Mn_{1.5}O_4$ lithium-ion battery cathodes prepared by a modified low temperature solution combustion synthesis, *Ceram. Int.,* **40**, 11611, (2014).

[18] Hong, C.S., Ravindranathan, P., Agrawal, D.K., *et al.*: Synthesis and sintering of amorphous cordierite powders by a combustion method, *J. Mater. Sci. Lett.,* **13**, 1361 – 1363, (1994).

[19] Shao, H., Liang, K., Zhou, F., Wang, G., Hu, A.: Microstructure and mechanical properties of $MgO$-$Al_2O_3$-$SiO_2$-$TiO_2$ glass-ceramics, *Mater. Res. Bull.,* **40**, 499 – 506, (2005).

[20] Dittmer, M., Müller, M., Rüssel, C.: Self-organized nanocrystallinity in $MgO$-$Al_2O_3$-$SiO_2$ glasses with $ZrO_2$ as nucleating agent, *Mater. Chem. Phys.,* **124**, 1083 – 1088, (2010).

[21] Dittmer, M., Yamamoto, C.F., Bocker, C., Rüssel, C.: Crystallization and mechanical properties of $MgO/Al_2O_3/SiO_2/ZrO_2$ glass-ceramics with and without the addition of yttria, *Solid State Sci.,* **13**, 2146 – 2153, (2011).

[22] Yang, C.F., Cheng, C.M.: The influence of $B_2O_3$ on the sintering of $MgO$-$CaO$-$Al_2O_3$-$SiO_2$ composite glass powder, *Ceram. Int.,* **25**, 383, (1999).

[23] Ruiz-Valdés, J.J., Gorokhovsky, A.V., Escalante-Garc, J.I., Mendoza-Suárez, G.: Glass-ceramic materials with regulated dielectric properties based on the system $BaO$-$PbO$-$TiO_2$-$B_2O_3$-$Al_2O_3$, *J. Eur. Ceram. Soc.,* **24**, 1505 – 1508, (2004).

[24] EI-Kheshen, A.A., Zawrah, M.F.: Sinterability, microstructure and properties of glass/ceramic composites, *Ceram. Int.,* **29**, 251 – 257, (2003).